JOURNAL OF PHYSIOLOGY AND PHARMACOLOGY 2014, 65, 4, 511-523
www.jpp.krakow.pl

A.J. ALEXANDROU[1,*], J.T. MILNES[2,3,*], S.Z. SUN[4], B. FERMINI[4], S.C. KIM[4], S. JENKINSON[7], D.J. LEISHMAN[5], H.J. WITCHEL[2,6], J.C. HANCOX[2*], J.L. LEANEY[8*]

THE HUMAN ETHER-A'-GO-GO RELATED GENE (hERG) K^+ CHANNEL BLOCKADE BY THE INVESTIGATIVE SELECTIVE-SEROTONIN REUPTAKE INHIBITOR CONA-437: LIMITED DEPENDENCE ON S6 AROMATIC RESIDUES

[1]Pfizer Neusentis, The Portway Building, Granta Park, Cambridge, CB21 6GS, United Kingdom; [2]School of Physiology and Pharmacolology, and Cardiovascular Research Laboratories, School of Medical Sciences, University Walk, Bristol, BS8 1TD, United Kingdom; [3]Current address: Xention Ltd, Iconix Park, London Road, Pampisford, Cambridge, CB22 3EG, United Kingdom; [4]Pfizer Inc., Global Safety Pharmacology, Eastern Point Road, MS 8274-1347, USA; [5]Lilly Research Laboratories, Indianapolis IN 46285, USA; [6]Current address: Brighton and Sussex Medical School, University of Sussex, Falmer BN1 9PX, United Kingdom; [7]Pfizer Inc., Global Safety Pharmacology, San Diego, CA 92121, USA; [8]Pfizer Inc., Discovery Park House, Ramsgate Road, Sandwich, Kent, CT13 9NJ, United Kingdom

Diverse non-cardiac drugs adversely influence cardiac electrophysiology by inhibiting repolarising K^+ currents mediated by channels encoded by the human *ether-a-go-go-related gene* (*hERG*). In this study, pharmacological blockade of hERG K^+ channel current (I_{hERG}) by a novel investigative serotonin-selective reuptake inhibitor (SSRI), CONA-437, was investigated. Whole-cell patch-clamp measurements of I_{hERG} were made from human embryonic kidney (HEK 293) cells expressing wild-type (WT) or mutant forms of the hERG channel. With a step-ramp voltage-command, peak I_{hERG} was inhibited with an IC_{50} of 1.34 μM at 35 ±1°C; the IC_{50} with the same protocol was not significantly different at room temperature. Voltage-command waveform selection had only a modest effect on the potency of I_{hERG} block: the IC_{50} with a ventricular action potential command was 0.72 μM. I_{hERG} blockade developed rapidly with time following membrane depolarisation and showed a weak dependence on voltage, accompanied by a shift of ~ –5 mV in voltage-dependence of activation. There was no significant effect of CONA-437 on voltage-dependence of I_{hERG} inactivation, though at some voltages an apparent acceleration of the time-course of inactivation was observed. Significantly, mutation of the S6 aromatic amino acid residues Y652 and F656 had only a modest effect on I_{hERG} blockade by CONA-437 (a 3–4 fold shift in affinity). CONA-437 at up to 30 μM had no significant effect on either $Na_v1.5$ sodium channels or L-type calcium channels. In conclusion, the novel SSRI CONA-437 is particularly notable as a gating-dependent hERG channel inhibitor for which neither S6 aromatic amino-acid constituent of the canonical drug binding site on the hERG channel appears obligatory for I_{hERG} inhibition to occur.

Key words: *human Ether-a'-go-go Related Gene, long QT, Torsade de Pointes, selective-serotonin reuptake inhibitors, cardiovascular, L-type calcium channels*

INTRODUCTION

Drug induced prolongation of the rate-corrected QT interval (QT_C-I) on the electrocardiogram (ECG) is associated with an increased risk of the potentially fatal arrhythmia, *Torsade de Pointes* (TdP); (1-3). As the incidence of TdP for QT_C-I prolonging drugs is generally rather low (2), surrogate markers of QT_C-I prolongation and TdP are generally used when testing the pro-arrhythmic propensity of novel chemical entities. The predictive accuracy of surrogate markers is a matter of great importance to drug development and safety (3, 4). A core component of pre-clinical cardiac safety testing, consistent with the S7B guidelines released by the International Conference on Harmonisation (ICH) is an *in vitro* electrophysiological assay to assess inhibitory effects of drugs on recombinant hERG K^+ channels (4, 5). hERG (*human ether-a-go-go-related gene*) is the cloned counterpart of channels responsible for the rapid delayed rectifier K^+ channel current 'I_{Kr}', which plays a key role in ventricular action potential repolarisation (6, 7). It is now widely accepted that the majority of cases of drug-induced QT prolongation are due to blockade of this channel by therapeutically and structurally diverse drugs (3, 4, 8). The high susceptibility of the hERG channel to pharmacological blockade is attributable in part to the channel's large inner cavity and in part to the presence of distinct aromatic amino-acid residues (Y652 and F656) in the S6 helices that facilitate drug binding (4, 8, 9).

Amongst the non-cardiac drugs now known to be associated with adverse cardiac events (10, 11) through modifying cardiac electrophysiology (12) and linked to acute pharmacological inhibition of hERG channels are antidepressants including the serotonin-selective reuptake inhibitors (SSRIs) fluoxetine (13-15), citalopram (14) and fluvoxamine (16). Citalopram and

[*] These authors contributed equally to this work

fluvoxamine have been shown to produce acute hERG channel current (I_{hERG}) inhibition that develops much more rapidly on membrane potential depolarisation than that produced by archetypal high affinity methanesulphonanilide hERG inhibitors such as dofetilide and E-4031 (14, 17, 18)). Fluvoxamine also appears to be particularly notable and unusual amongst identified hERG inhibitors (16) in that mutation of S6 aromatic residues only partially attenuates the potency of its very rapidly developing hERG channel blockade (16). The extent to which fluvoxamine is representative of other SSRIs in this regard is unclear, however, as fluoxetine inhibition of I_{hERG} has been shown to be markedly reduced by mutation of F656 (15). CONA-437 [4-(3-methoxy-4-methylsulfanyl-phenoxy)-pyridin-3-ylmethyl]-dimethyl-amine is an investigative SSRI that preliminary tests have indicated exerts rapidly developing I_{hERG} inhibition (19). The present study was conducted in order to characterise in detail the time-, voltage- and protocol-dependence of acute I_{hERG} inhibition by CONA-437 and to establish the sensitivity of the drug's hERG channel inhibition to mutation of the Y652 and F656 S6 aromatic residues. The results of the study establish CONA-437 to be a gating-dependent inhibitor of hERG channels that shows a comparatively limited dependence of inhibition on interactions with S6 aromatic amino-acid residues.

MATERIALS AND METHODS

Cell culture

Human embryonic kidney 293 cells stably expressing hERG

Human embryonic kidney (HEK) 293 cells stably expressing hERG1a (K_v11.1a), were obtained from Dr. Craig. T. January (University of Wisconsin) (20). The creation of HEK 293 cell lines stably expressing the S6 mutations F656A and Y652A to hERG1a has been described previously (16). Cells were maintained using minimum essential medium with Earle's salts (MEM) supplemented with 10% foetal calf serum, 2 mM L-glutamine, 1 mM sodium pyruvate, 1× non-essential amino acids and 0.4 mg.ml^{-1} Geneticin (G-418) and kept at 37°C in a humidified atmosphere of 5% CO_2. For patch clamp experiments, cells were plated onto glass coverslips placed in 30 mm Petri dishes and used within 72 hours of plating.

Chinese hamster ovary cells stably expressing $Na_v1.5$

Chinese hamster ovary (CHO) cells stably transfected with the human SCN5A gene, which encodes $Na_v1.5$ channels, were obtained from ChanTest Corporation. The cell line was grown in Ham's F-12 with L-glutamine with 10% foetal bovine serum, 2% Penicillin-Streptomycin, and 0.5% Geneticin, and was maintained at ~37°C in a humidified atmosphere containing 5% CO_2. The cells were passaged every 3–5 days based on confluence. On the day of the experiment, 80–100% confluent cells were harvested from a 175 cm^2 culture flask using Detachin™. After 10 minutes of exposure to Detachin™ at 37°C, the cells were centrifuged for 2 minutes at 1000 RPM. The supernatant was removed and the cell pellet was reconstituted in 5–8 ml of serum free media with 2.5% of 1 M HEPES and placed on the Qstirrer™ and allowed to recover. After a ~30 minute recovery period, experiments were initiated.

H9C2 cells

The rat cardiac H9C2 cell line was utilized in a L-type calcium channel assay (ATCC; Cat # CRL-1446). H9C2 cells were grown in DMEM containing 10% (v/v) heat-inactivated foetal bovine serum (FBS). Cells were expanded, harvested using TrypLE, resuspended in the same media containing 10% (v/v) DMSO and were frozen at a concentration of 5 million per ml at a rate of –1°C/minute (until –80°C).

hERG electrophysiology

Cells were continuously superfused with extracellular solution (ECS) of the following composition (mM): NaCl 130; KCl 4; $CaCl_2$ 2; $MgCl_2$ 1; glucose 10; HEPES 5; (titrated to pH 7.4 with NaOH). In ECS containing elevated potassium ($[K^+]_o$), elevated K^+ was compensated for by a corresponding reduction in external Na^+, such that the concentration of KCl was 94 mM and NaCl was 50 mM (21, 22). The patch pipette (intracellular) solution (ICS) contained (in mM): KCl 130; MgATP 5; $MgCl_2$ 1; HEPES 10; EGTA 5; (titrated to pH 7.2 with KOH). Liquid junction potential values were calculated of +4.8 mV and –1.8 mV in standard ECS/ICS and high K^+ ECS/ICS (JPCalc); (23). As these values were small, no corrections were performed. When filled with ICS, the patch pipettes had a tip resistance of 1.5–4 MΩ. Whole-cell patch clamp recordings of membrane currents were made using either a Multiclamp 700A or an Axopatch 200B amplifier (Axon Instruments Molecular Devices Corporation, Foster City, CA). Currents were filtered at 1 kHz, digitised at 5 kHz (unless otherwise stated) and data acquired using either a Digidata 1322A (used with a Multiclamp 700A amplifier) or a Digidata 1200 (used with an Axopatch 200B amplifier). The pClamp suite of software (versions 8 and 9.2; Axon Instruments Molecular Devices Corporation) was used to generate voltage clamp protocols, acquire data and analyse current traces. Series resistance compensation was routinely applied to at least 75% and tips of pipettes were coated in a parafilm and mineral oil emulsion to reduce stray capacitance. On achieving the whole-cell configuration, pulses were repeatedly applied until stable evoked current responses were obtained; experiments then commenced. A control period was recorded in ECS and then CONA-437 was applied until steady state effects were achieved. All experiments were carried out at 35 ±1°C, unless otherwise stated.

$Na_v1.5$ electrophysiology

$Na_v1.5$ current was elicited and recorded using the automated QPatch HT™ system. The suspended cells in the Qstirrer™ were transferred to 48 individual recording chambers on a QPlate 48™ containing extracellular recording saline composed of (in mM): NaCl 138, KCl 5.3, $CaCl_2$ 1.3, $MgCl_2$ 0.5, glucose 5.6, HEPES 5, $MgSO_4$ 0.4, KH_2PO_4 0.44, $NaHCO_3$ 4.2, Na_2HPO_4 0.34 adjusted to pH 7.4 ±0.1 with NaOH. Membrane currents were measured at room temperature (~22°C) using the QPlate 48™ electrode array, filled with intracellular recording saline composed of (in mM): 130 KCl, 1 $MgCl_2$, 10 HEPES, 5 Mg-ATP, and 5 EGTA; adjusted to pH 7.2 ±0.1 with KOH.

$Na_v1.5$ current (I_{Na}) was elicited with a voltage step to –20 mV for 30 ms from a holding potential of –80 mV. Test pulses were delivered at a frequency of 1 Hz. At least 5 minutes of control recordings were performed prior to the first exposure of the cell to test compound. Four drug concentrations were tested on each cell, each exposure lasting 5 minutes or until steady-state effects were observed. The Class Ic antiarrhythmic drug propafenone was employed as a positive control.

Cell based functional L-type calcium channel assay

Calcium channel activity was measured in the cardiac H9C2 cell line which was maintained in Dulbecco's Modified Eagle Medium containing 10% (v/v) heat-inactivated foetal bovine serum and glutamine (2 mM). Cells were plated into 384-well

black, clear-bottom tissue culture treated plates (Greiner, Germany) at a density of 5000 cells per well (100 µl) and were left to grow for 72 hours prior to the start of the experiment.

Media was removed from the plates and 20 µl of Hank's balanced salt solution (Invitrogen, USA) containing 20 mM HEPES and Calcium-5 dye (Molecular Devices, USA) was added to each well. The plates were returned to the incubator for 1 hour to allow dye loading. Subsequently, 5 µl of compound or vehicle was added to each well. Following a further 15 min incubation at room temperature, the plate was transferred to a FLIPR® Tetra fluorescent plate reader. 25 µl of a KCl buffer (KCl, 140 mM; $MgCl_2$, 1 mM; HEPES, 20 mM; glucose, 10 mM, $CaCl_2$, 10 mM) was added to each well using the FLIPR to depolarize the cells. The real-time change in fluorescence was measured every second for a total of 120 s. The dihydropyridine L-type Ca^{2+} channel blocker nifedipine was employed as a positive control.

Data analysis

Data were analysed using Clampfit v9.2 (Axon Instruments Molecular Devices Corporation), QPatch assay software v5.0, Excel 2000 (Microsoft) and Origin v.6.0 (Microcal) software. Data are presented as mean ± S.E.M. with the exception of IC_{50} and n_H, which are expressed as mean and 95% confidence intervals (CI). n denotes the number of cells recorded from or wells (plate-based Ca^{2+} assay). Statistical comparisons were made using a two-tailed Student's t-test or one-way analysis of variance (ANOVA) with a Bonferroni post test (* indicates P≤0.05, ** indicates P≤0.01 and *** indicates P≤0.001).

Drugs and reagents

CONA-437 [4-(3-methoxy-4-methylsulfanyl-phenoxy)-pyridin-3-ylmethyl]-dimethyl-amine was dissolved in DMSO to

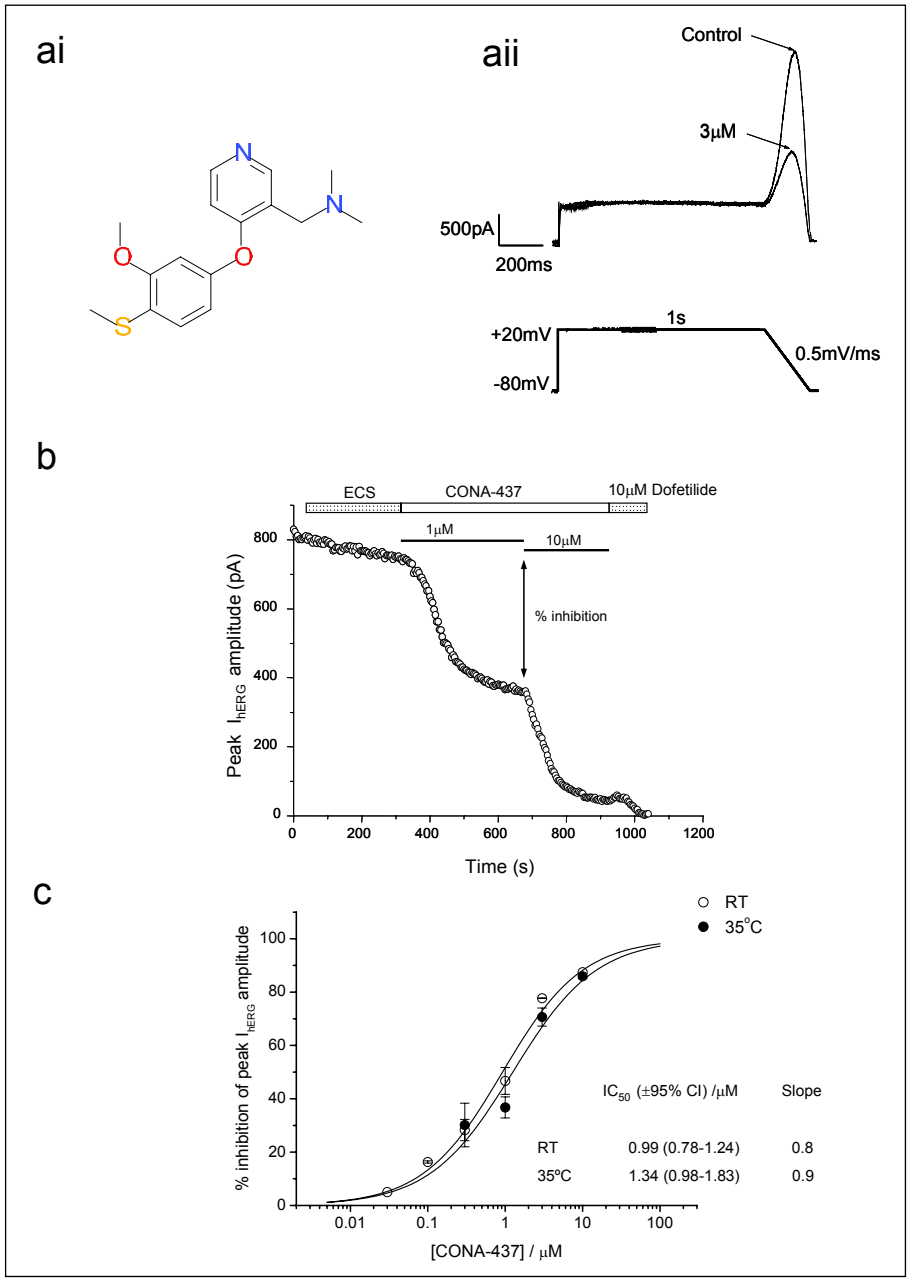

Fig. 1. Dose-dependence of CONA-437 I_{hERG} inhibition is temperature-independent.
(a) (ai) shows chemical structure of CONA-437. (aii) 'Step-ramp' voltage command used to evoke hERG currents. Peak hERG current amplitude in control conditions and in the presence of 3 µM CONA-437 was measured during the repolarising phase as indicated in the example traces shown.
(b) This graph illustrates the effects of cumulative concentrations of CONA-437 (1 and 10 µM) on peak hERG amplitude with time. Dofetilide (10 µM) was added at the end of the experiment as a positive control.
(c) Cumulative concentration–response curves to CONA-437 at RT and at 35 ±1°C. Data are shown fitted to a Hill equation of the form $y=[(A_1-A_2)/(1+(x/C)^{nH})]+A_2$ where A_1 and A_2 are 0 and 100% inhibition, respectively, C is the IC_{50} concentration and n_H is the Hill coefficient (n=2–7 cells per concentration).

prepare a stock solution of 10 mM. Further dilutions were then made in DMSO to give the desired test concentrations with a final DMSO concentration of 0.1%. Dofetilide was prepared as a 10 mM stock solution in DMSO and diluted down to a final concentration of 10 μM. Solutions were either made up fresh each experimental day or small aliquots were stored at –80°C and defrosted only once. CONA-437 and dofetilide were both synthesised in house at Pfizer Inc. Propafenone and nifedipine were purchased from Sigma-Aldrich. Tissue culture reagents were obtained from Invitrogen or Sigma-Aldrich.

RESULTS

Dose-dependence of CONA-437 inhibition of I_{hERG} is temperature-independent

A 'step-ramp' protocol identical to that used in prior I_{hERG} pharmacology studies from our laboratories (24, 25) was used to evoke I_{hERG} in control conditions and in the presence of CONA-437, as illustrated in *Fig. 1a.* Cells were voltage-clamped at –80 mV and depolarised to +20 mV for 1 s followed by a repolarising ramp back to –80 mV at a rate of 0.5 mV/ms. The voltage command was applied every 4 s. I_{hERG} was measured both at the end of the depolarising step and as peak current during the repolarising ramp phase of the voltage protocol. The effects of CONA-437 on I_{hERG} when recording at 35 ±1°C were compared to those on currents recorded at room temperature (~22°C). To establish a concentration-response relationship, increasing concentrations of CONA-437 were cumulatively applied to the bath until steady-state effect was achieved (24). A supra-maximal concentration of dofetilide (10 μM) was also applied at the end of each experiment as a positive control (*Fig. 1b*) (24). Dofetilide is known to become trapped in I_{Kr}/hERG channels with poor recovery of block at negative voltages (26). CONA-437 washout was therefore not investigated in this study. For each concentration of CONA-437, steady-state percentage inhibition was evaluated when 3 consecutive sweeps were superimposed on one another (24). Mean percentage block values were calculated for both depolarising step and peak I_{hERG} at each concentration. There was no significant difference between mean % block of depolarising step and peak I_{hERG} currents at each concentration of CONA-437 (data not shown). Concentration-response curves were constructed for peak I_{hERG}, and a Hill equation fitted to the data, yielding an IC_{50} of 1.34 μM (95% CI: 0.98–1.83 μM) and a Hill coefficient (n_H) of 0.9 at 35 ±1°C and an IC_{50} of 0.99 μM (95% CI: 0.78–1.24 μM) and n_H of 0.8 at room temperature (*Fig. 1c*). The derived IC_{50} values at the

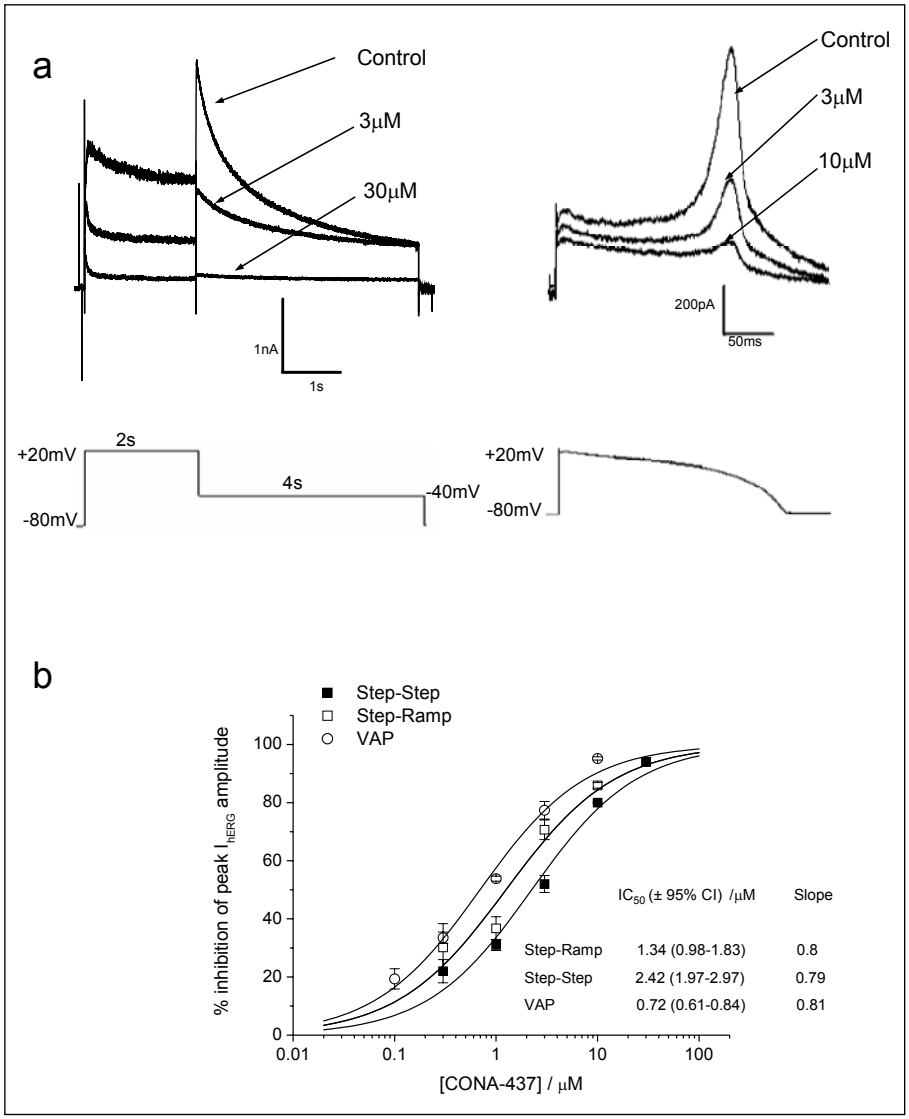

Fig. 2. Potency of CONA-437 is influenced by different voltage waveforms.
(a) This panel illustrates an example of currents evoked using either the "step-step" voltage protocol or a ventricular action potential (VAP) waveform. Voltage commands were applied every 12 s and multiple concentrations of CONA-437 were cumulatively bath-applied to each cell as in Fig. 1b. Example current traces elicited using these waveforms are shown, and the effect of CONA-437 on peak hERG tail currents was measured.
(b) Concentration-response curves using the 'step-step' and VAP protocols are shown with the 'step-ramp' dose-response (at 35±1°C) curve for comparison. As in *Fig. 1c*, data were fitted to a Hill equation where % inhibition was constrained between 0 and 100%. Values for IC_{50} and n_H are indicated (n=2–13 cells per concentration).

two temperatures were not statistically significantly different from one another (P=0.84).

Comparison of potency of I_{hERG} inhibition by CONA-437 between different voltage waveforms

There is evidence that the observed potency of some hERG inhibiting drugs in electrophysiological experiments is influenced by the voltage protocol used (25, 27-29). In order to determine whether or not this is the case for CONA-437, we conducted experiments using different voltage commands to stimulate hERG channels. Thus, in addition to the step-ramp protocol employed in *Fig. 1*, we used a 'step-step' protocol where cells were depolarised from a holding potential of –80 mV to +20 mV for 2 s followed by a 4 s step to –40 mV to elicit outward I_{hERG} tails: this was applied every 12 s (*Fig. 2a*; left-hand panel). We also applied a physiological ventricular action potential (VAP) waveform recorded from guinea pig papillary muscle to elicit hERG currents (*Fig. 2a*; right-hand panel). The effects of CONA-437 on the peak I_{hERG} tails were measured and concentration-response relationships generated, as illustrated in *Fig. 2b*. We observed small, although not statistically significant, differences in potency using differing voltage protocols (VAP, IC_{50}: 0.72 μM, (95% CI: 0.61–0.84), n_H 0.81; "step-step" protocol, IC_{50}: 2.42 μM, (95% CI: 1.97–2.97), n_H 0.79), compared to that generated using the "step-ramp" protocol. I_{hERG} tails elicited by the step-step protocol in *Fig. 2a* were fitted with a bi-exponential function to obtain fast and slow time-constants of deactivation (τ_f and τ_s, respectively) in the absence and presence of 3 μM CONA-437. τ_f was 161.4±32.9 ms in control and 226.8 ±34.3 ms in CONA-437 ($p<0.05$), whilst τ_s was similar in control and CONA-437 (1222 ±80 ms and 1138 ±82 ms respectively; no significant difference). Thus, the fast component of deactivation became slower in the presence of CONA-437, without any change to the slower component.

CONA-437 inhibition of hERG current is weakly voltage-dependent

The effect of CONA-437 on voltage-dependence of I_{hERG} activation was investigated by applying depolarising voltage steps of 2 s duration from a holding potential of –80 mV to a range of test potentials starting at –60 mV and increased in 10

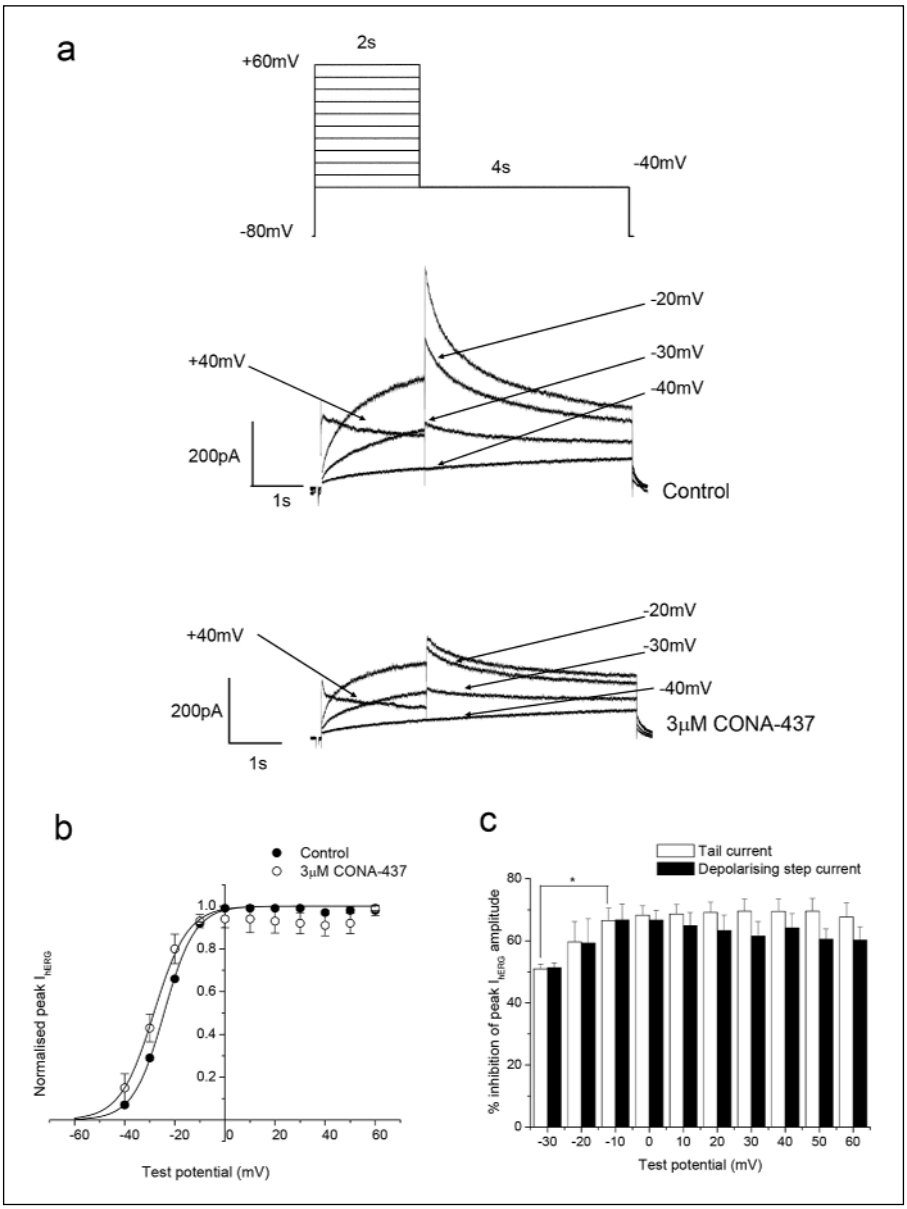

Fig. 3. CONA-437 inhibition of hERG currents is weakly voltage dependent.
(a) Upper panel shows the voltage command used. The lower panels show representative examples of current traces recorded in the absence and presence of 3 μM CONA-437. For clarity not all current traces are shown.
(b) Activation curves for tail currents in control and in the presence of 3 μM CONA-437. Peak tail currents for each individual cell were normalised to the maximum obtained in the absence of drug, and fitted with a Boltzmann function of the form $y=[(A_1–A_2)/(1+e^{(x–V1/2)/k}]+A_2$ where A_1 and A_2 are 0 and 1 respectively, $V_{1/2}$ is the half-activation voltage and k is the slope factor. The $V_{1/2}$ and k values indicated are the mean from 4 cells.
(c) Magnitude of I_{hERG} inhibition by 3 μM CONA-437 at various test potentials. Inhibition of depolarising step currents is indicated by the solid bars and tail currents by the open bars.

mV increments (*Fig. 3a*). Some I_{hERG} blocking compounds exhibit a clear voltage-dependence illustrated by a shift in channel activation and $V_{1/2(act)}$ values. It has been reported in some studies that a time-dependent shift in channel activation may occur in the absence of drug (16, 30). Consequently, sufficient time (at least 6 minutes) was allowed to elapse to ensure stable current-voltage relationships to be recorded, thus allowing the study of possible effects of CONA-437 on voltage-dependent activation, independent of time-dependent changes.

We measured depolarising step I_{hERG} amplitudes and peak I_{hERG} tails upon repolarisation to –40 mV in the absence and presence of 3 μM CONA-437. Representative examples of current traces are shown in *Fig. 3a*. Current-voltage (I-V) relationships for both depolarising step and peak tail currents were plotted; *Fig. 3b* shows, the I-V relationship for peak I_{hERG} tails. The peak tail current data obtained from individual cells were fitted to a Boltzmann function and $V_{1/2(act)}$ and slope factors were derived. The mean $V_{1/2(act)}$ was –24.3 ±0.3 mV under control conditions and in the presence of CONA-437 was significantly shifted to –29.3 ±1.5 mV (n=4, P=0.04) whilst the slope factors in control and drug were not significantly different: 6.1±0.1 mV and 5.8±0.4 mV, respectively (P=0.59). *Fig. 3c* shows the magnitude of inhibition of peak tail and depolarising step currents by 3 μM CONA-437 at different test potentials. At –30 mV, significant block of tail currents was observed (40.4 ±10.6%; n=4). The extent of block was significantly enhanced as the membrane became more depolarised and reached a plateau level at –10 mV (66.6±7.9%; P<0.05) suggesting that block is weakly voltage-dependent. Furthermore, the extent of inhibition of depolarising step currents also exhibited weak voltage-dependence.

Time-dependence of hERG inhibition by CONA-437

In order to investigate the time-dependence of CONA-437 block of I_{hERG}, we used a long duration voltage-command to ascertain whether inhibition was maintained during sustained depolarisation. Cells were stepped to 0 mV for 10 s from a holding potential of –80 mV and a control current was recorded in the absence of CONA-437. Membrane potential was then held at –80mV whilst CONA-437 was applied, and after 5 minutes in CONA-437 in the absence of pulsing the protocol was then

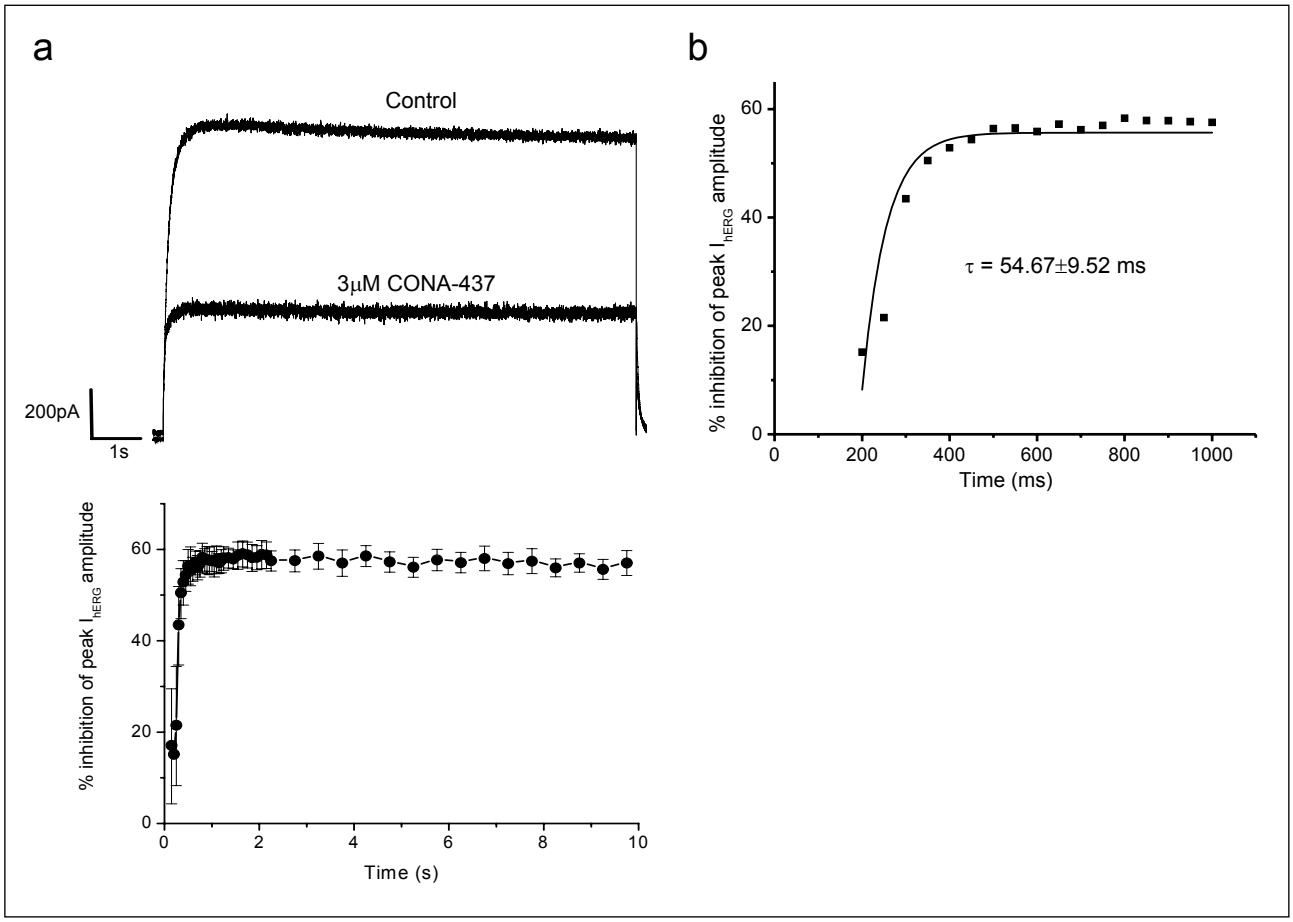

Fig. 4. Time-dependence of hERG blockade by CONA-437.
(a) Cells were depolarised from the holding potential of –80 mV to 0 mV for 10 s. This voltage command was repeated until a steady-state response was observed. 3 μM CONA-437 was then bath-applied for 5 minutes whilst the channels were voltage clamped at –80 mV. The voltage command was then again repeated in the presence of CONA-437. The representative traces in the upper panel indicate the last pulse prior to, and the first pulse during application of 3 μM CONA-437. The lower panel shows mean development of block over time by 3 μM CONA-437 from 4 experiments. Full block was observed within less than 1 s and was maintained for the 10 s duration.
(b) Development of block during the first second of the pulse from a representative cell. Each individual experiment was fit by a single exponential yielding an overall mean tau of 54.7±9.5 ms.

repeated (*Fig. 4a*, upper panel). Block of I_{hERG} was observed during the step to 0 mV (*Fig. 4a*; lower panel) and the extent of block did not change with application of subsequent long depolarisations (data not shown). I_{hERG} block developed rapidly within the first 1 second of the pulse (*Fig. 4b*) and could be fit to a single exponential function. A single exponential fit to the development of block in each of the 4 experiments yielded a mean τ value of 54.7±9.5 ms (n=4). We used an ANOVA to examine whether the development of block was time-dependent and found that at later time points (>1s) the degree of block was significantly greater suggesting that block was time-dependent. Analysis of the data demonstrated that block exhibited significant time-dependence (P=0.001). The extent of block at various time points during the entire 10 seconds depolarising step was calculated for 3 µM CONA-437 and was found to remain constant between 1 and 10 s (*Fig. 4a*, lower panel). Time-dependent inhibition of I_{hERG} during this protocol was accompanied by acceleration of development of the current on depolarisation: in five further experiments the time-to-peak of I_{hERG} following depolarisation to 0 mV was 479.2 ±69.8ms in control and 201.9±3.0 ms in CONA-437. This may reflect acceleration of I_{hERG} activation in the presence of the drug and/or the consequences of time-dependent inhibition.

To investigate further the time-dependence of block by CONA-437 at the shorter pulse durations, cells were depolarised to +40 mV for either 30 or 200 ms from a holding potential of –80 mV and I_{hERG} peak tail currents were observed on repolarisation to –40 mV. This protocol was applied under control conditions and after a 5 minute application of 3 µM CONA-437 whilst cells were voltage-clamped at –80 mV. *Fig. 5a* shows the currents obtained and the corresponding voltage commands. The amplitude of tail currents evoked at –40 mV was measured in the absence and presence of 3 µM CONA-437 and the effects of drug expressed as percentage inhibition of peak tail currents (*Fig. 5b*). We observed that 3 µM CONA-437 produced a significant attenuation of I_{hERG} even after only a 30 ms depolarising step (35.8±5.1%, n=5, P=0.001) and that inhibition was significantly increased as pulse duration was increased (P<0.02).

Effects of CONA-437 on I_{hERG} inactivation

Data from the experiments described above provide evidence that CONA-437 blockade of I_{hERG} in a manner consistent with rapid gating-dependent inhibition, with the presence of significant inhibition with brief (30 ms) depolarisation also raising the

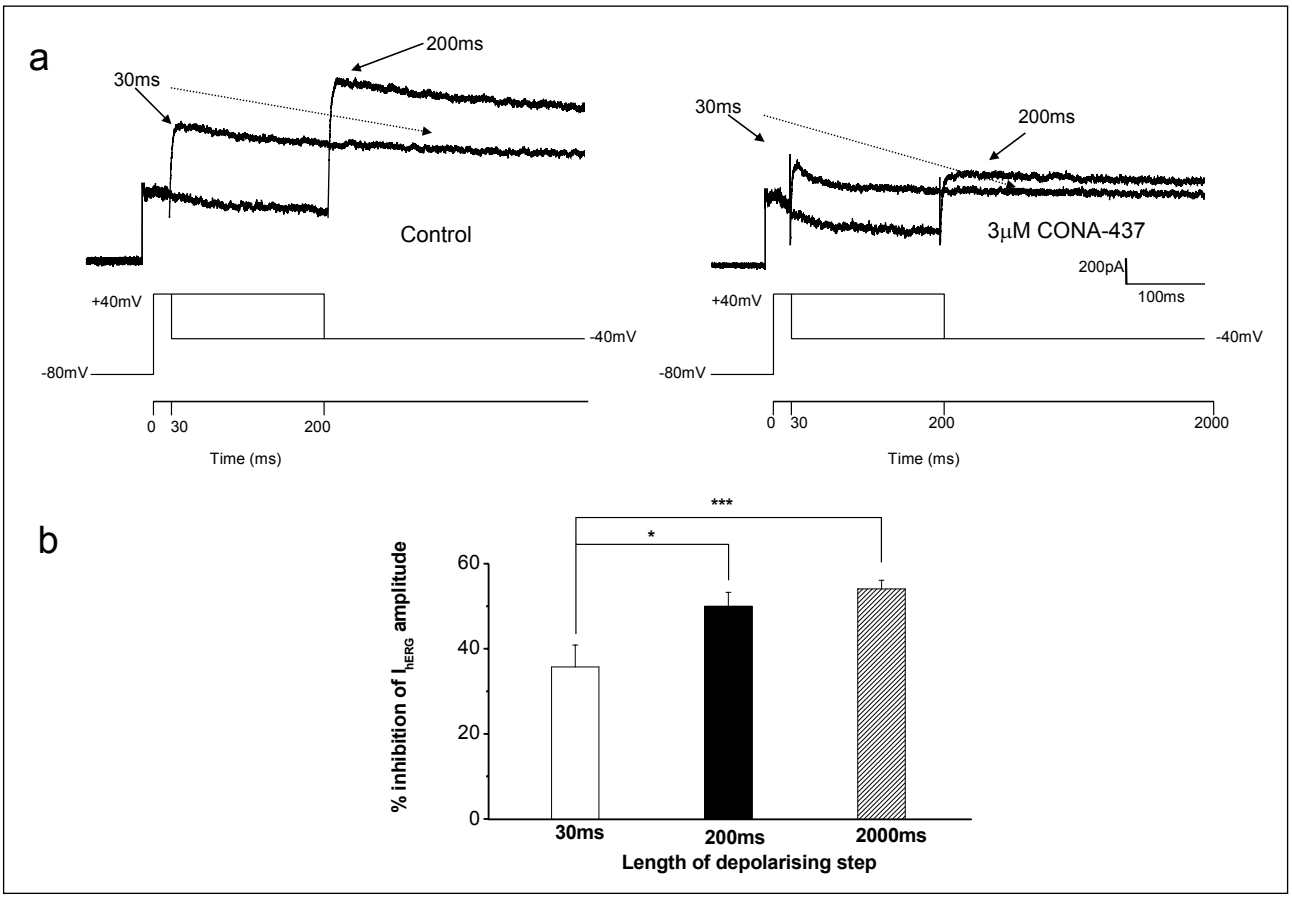

Fig. 5. State-dependence of hERG blockade by CONA-437.
(a) Cells were briefly depolarised from a holding potential of –80 mV to +40 mV for either 30 or 200 ms before repolarising to –40 mV to elicit tail currents. Peak tail currents were measured in control conditions and after equilibration of cells in 3 µM CONA-437, whilst cells were voltage-clamped at –80 mV. The representative traces show the increase in peak tail current with duration of the depolarising step in the absence (left hand traces) and presence (right hand traces) of CONA-437.
(b) Summary of mean data from these experiments (n=4–12 cells) where mean % inhibition of peak tail currents is plotted as a function of pulse duration. With a 30 ms step, 35.8±5.1% inhibition was achieved. As pulse duration was lengthened, inhibition was significantly increased (200 ms: 50.0±2.39%; P=0.018).

possibility of a component of closed channel block. To investigate further the state-dependence of CONA-437 block of I_{hERG} we examined the agent's effect on inactivation kinetics of I_{hERG} using two additional voltage protocols. With the first of these, we examined whether CONA-437 had any effects on the voltage-dependence of hERG current inactivation. Cells were depolarised to +40 mV for 500 ms from a holding potential of –80 mV, 2 ms pulses were then applied to test potentials between –140 mV and +30 mV in 10 mV increments, followed by a second 500 ms step to +40 mV. I_{hERG} elicited during the final depolarising step to +40 mV was measured and normalised to the maximum current observed. The normalised values were then plotted as a function of test potential to generate steady-state inactivation relations for each cell in the absence and presence of CONA-437 (3 μM) and $V_{1/2(inact)}$ values calculated. *Fig. 6a* upper panel shows representative currents in control and CONA-437, focusing on current elicited during the second step to +40 mV following the ladder of brief repolarising steps (shown as an inset to *Fig. 6a*). Mean inactivation relations in the absence and presence of CONA-437 (3 μM) are also shown in *Fig. 6a*: CONA-437 had no statistically significant effect on the mean $V_{1/2(inact)}$ values (–59.3 ±9.2 mV and –59.2 ±4.5 mV, n=4, respectively) or on the slope factors for the relation (18.7 ±1.3 mV and 20.6 ±1.2 mV, respectively). In experiments to examine the effects of CONA-437 on the time course of I_{hERG} inactivation, we used a voltage protocol which allowed us to measure time constants of inactivation at different test potentials. Cells were depolarised to +50 mV for 500 ms from a holding potential of –80 mV and then briefly (2 ms) stepped to –100 mV followed by a subsequent step to test potentials ranging from –50 mV to +50 mV. Representative current traces in the absence and presence of 3 μM CONA-437 are shown in *Fig. 6b* (upper panel). For each test potential, the time-

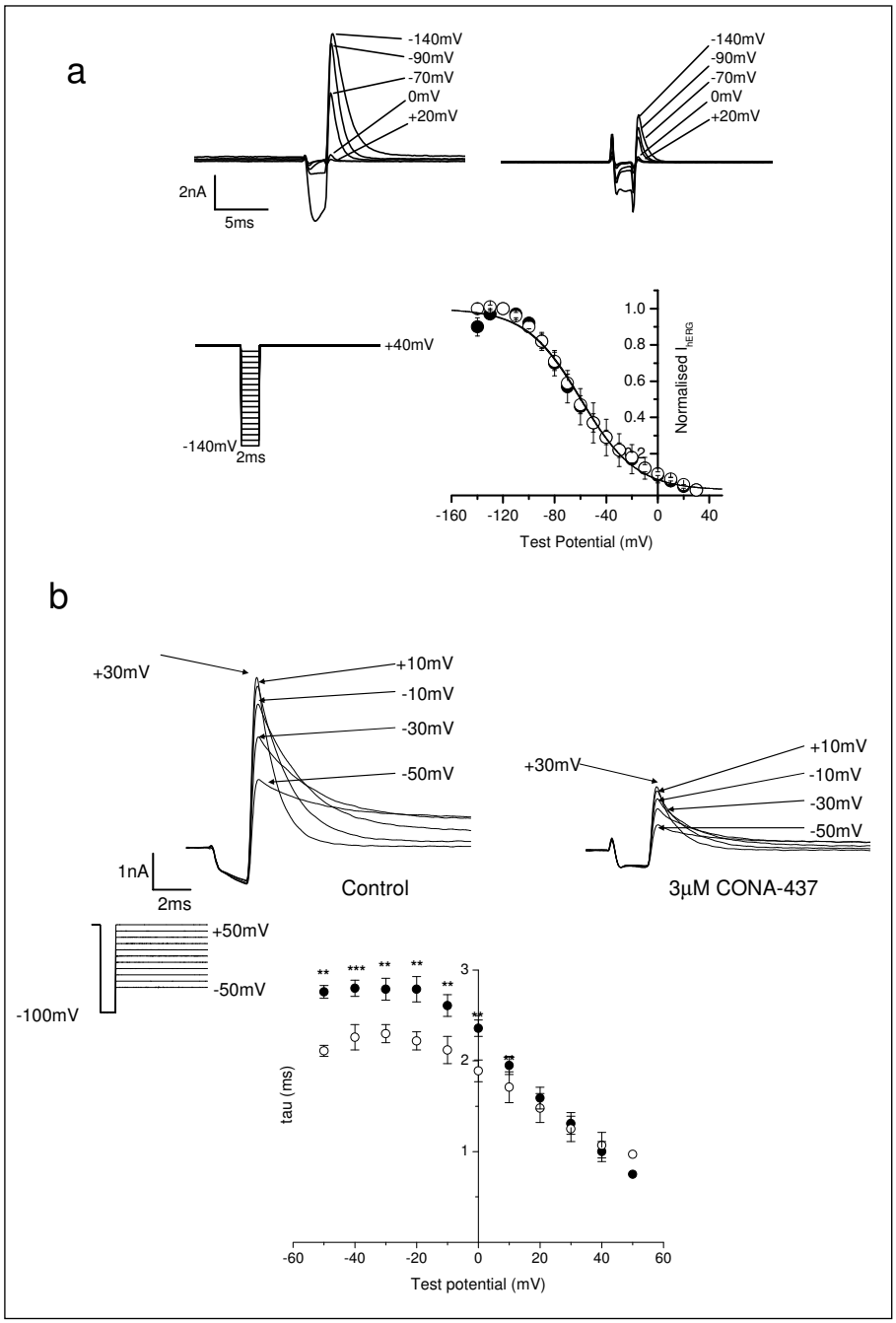

Fig. 6. Effects of CONA-437 on hERG current inactivation.
(a) Following a 500 ms step to +40 mV, 2 ms pulses were applied to potentials between –140 mV and +30 mV in 10 mV increments, followed by a second 500 ms step to +40 mV (inset). Example of current recordings was displayed at the top (control on the left, and 3 μM CONA-437 on the right). Current amplitudes elicited during the final step to +40 mV were measured, normalised and plotted as a function of the preceding test potential to yield a steady-state inactivation curve. This experiment was conducted under control conditions (in filled circles) and in the presence of 3 μM CONA-437 (in open circles). The mean $V_{1/2(inact)}$ under control conditions was –59.3 ±9.2 mV (slope 18.7 mV) and in the presence of CONA-437, –59.2±4.5 mV (slope 20.6 mV).
(b) Example traces in the upper panel illustrate the effects of CONA-437 on inactivation kinetics. Cells were depolarised to +50 mV for 500 ms and then briefly stepped to –100 mV followed by a subsequent step to test potentials ranging from –50 mV to +50 mV (inset). For clarity not all current traces are shown. The outward currents elicited during this final step were then fitted to a single exponential function to yield a time constant at each test potential. Time constants were then plotted versus test potential as shown in the lower part of this panel (n=4 cells).

course of inactivation of I_{hERG} elicited during the second depolarising step was fitted to a single exponential function yielding inactivation time constants at each test potential, in the presence and absence of drug. We found that CONA-437 significantly accelerated the time course of inactivation at potentials more negative than, and including, +10 mV (*Fig. 6b*, lower panel).

Using S6 helix mutants to investigate block of the hERG channel by CONA-437

In order further to understand the mechanism of I_{hERG} block by CONA-437 we examined the effects of mutations of the pore-S6 aromatic amino acid residues, Tyr652 and Phe656 to alanine residues (Y652A and F656A). For these experiments we used HEK 293 cell lines stably expressing either hERG-Y652A or hERG-F656A as previously described (16, 24). The Y652A mutant was tested using the standard 'step-step' protocol as described in *Fig. 2* and we used a drug concentration which would produce very extensive blockade of wild-type (WT) hERG channels (applying 30 μM CONA-437; >10-fold the IC_{50} value for WT I_{hERG} in *Fig. 2*). Representative current traces, as shown in *Fig. 7a*, indicate the effects of 30 μM CONA-437 on WT-hERG channels (left-hand panel) and on Y652A channels (right-hand panel). For the WT-hERG channels 30 μM CONA-437 produced 94 ±1.4% inhibition of I_{hERG} (n=3) compared to 48±6.1% inhibition in cells transfected with the Y652A channel (n=6), an IC_{50} value was estimated for the block of Y652A channels of 33.6 μM, an approximate three-fold shift in potency. We also examined the effects of CONA-437 on F656A hERG channels. For these experiments we used 94 mM external K^+ in order to maximise current carried by the low expressing F656A mutant, as previously reported (16, 24). Currents were evoked using a modified 'step-step' protocol where cells were repolarised from +20 mV to –120 mV for 500 ms prior to returning membrane potential to –80 mV; inhibition of peak I_{hERG} was measured for inward tail currents at –120 mV. We found that measuring tail currents at –120 mV in high external K^+ (94 mM) dramatically attenuated block of WT-hERG channels, 30 μM CONA-437 caused approximately 50% inhibition of I_{hERG} (data not shown). To determine whether the inward tails or high external K^+ ($[K^+]_e$) is responsible for attenuated block of the WT-hERG channels, we carried out similar

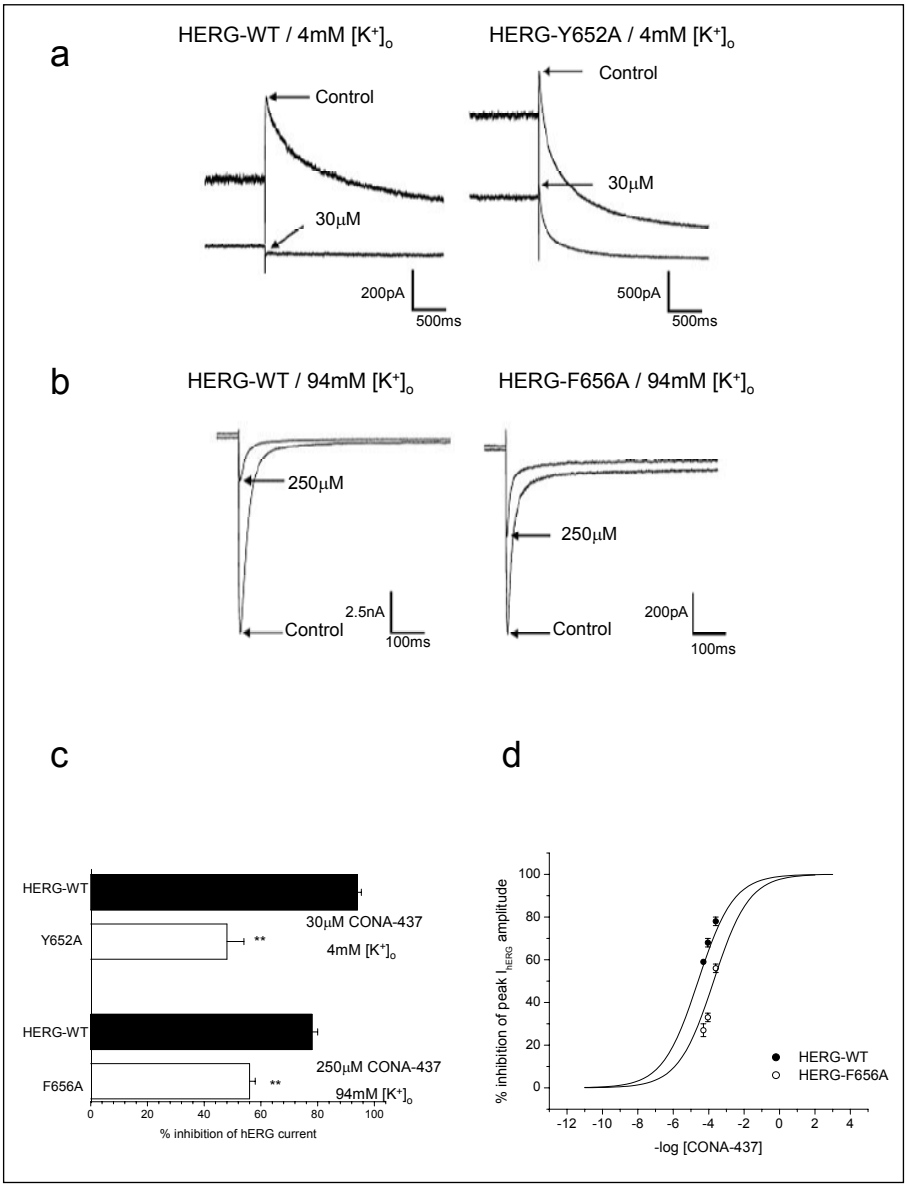

Fig. 7. Partial attenuation of CONA-437 block by F656A and Y652A.
(a) Representative current traces showing the effects of a maximal concentration of CONA-437 (30 μM) on WT channels (left) and on Y652A channels (right). Experiments were performed in the presence of 4 mM external K^+ and the voltage protocol is shown as an inset.
(b) Currents were evoked using a modified 'step-step' protocol (see inset). Representative current traces shown indicate the effects of a maximal concentration of CONA-437 (250 μM) on WT channels (left) and on F656A channels (right). Experiments were performed in the presence of 94 mM external K^+ to maximise the low expression of the F656A mutant (hence, inward tail currents).
(c) Magnitude of I_{hERG} inhibition by CONA-437 for the mutants tested, compared to the effects on the WT channel.
(d) Concentration - response curve to CONA-437 for hERG-WT and hERG- F656A channels in 94 mM external K^+. Data are shown fitted to a Hill equation (as described in the legend to *Fig. 1*).

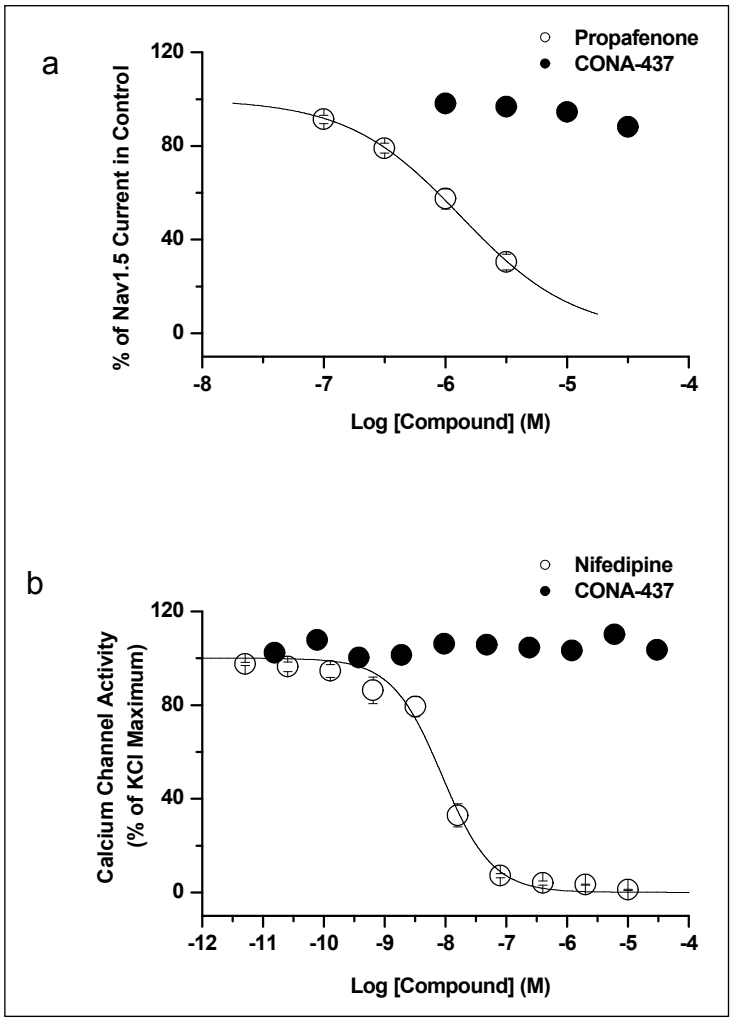

Fig. 8. Effects of CONA-437 on I_{Na} and L-type Ca^{2+} channel activity.
(a) Effects of CONA-437 and the positive control propafenone on $Na_v1.5$ currents were plotted against test concentrations. CONA-437 did not have any significant effect on $Na_v1.5$ current at all concentrations tested (n=4), whereas the positive control propafenone produced a concentration-dependent inhibition of $Na_v1.5$ with an IC_{50} of 1.30 μM.
(b) Summary data of L-type Ca^{2+} channel activity by CONA-437 and the positive control of nifedipine were plotted. While the positive control showed a concentration-dependent inhibition of L-type Ca^{2+} channel activity with an IC_{50} of 8.7 nM, CONA-437 displayed no effect at up to 30 μM.

experiments in ECS (4 mM K^+). 30 μM CONA-437 caused 73.7 ±3.8% inhibition of I_{hERG} (data not shown). This attenuation of block in high K^+ is similar to that observed previously for other drugs including fluvoxamine, E-4031, amiodarone and dronedarone (31, 32) and is consistent with drug displacement with increased inward flux of K^+ ions.

Due to the effect of raised $[K^+]_e$ on CONA-437 blockade of inward I_{hERG}, for subsequent experiments we used a higher CONA-437 concentration of 250 μM. The representative current traces in *Fig. 7b* illustrate the effects of 250 μM CONA-437 on WT channels (left-hand panel) and on F656A channels (right-hand panel). In the WT channels 250 μM CONA-437 produced 77 ±2.1% inhibition of I_{hERG} (n=6) compared to 56±2.1% inhibition in cells transfected with the F656A channel (n=8). The data for experiments using Y652A and F656A cell lines are summarised in the bar-chart in *Fig. 7c*. We generated a concentration-response curve to CONA-437 in 94mM external K^+ for both WT-hERG and F656A channels. We observed a significant decrease in potency of CONA-437, as shown in *Fig. 7d* (right-hand panel), with IC_{50} values of 41.4 μM (95% CI: 29.1–58.9 μM) and 176 μM (95% CI: 143–217 μM) on hERG-WT and F656A mutant channels, respectively (an approximate 4-fold change in potency).

Effects on $Na_v1.5$ and L-type Ca^{2+} channels

Some hERG blocking compounds exert mixed ion channel blocking effects (MICE) that, if on inward cation currents (L-type Ca^{2+} current, I_{Na}), could feasibly offset hERG-mediated drug actions on cardiac repolarisation; indeed, a recent study has provided evidence that comparison of concentration-response data on hERG with data on $Ca_v1.2$ and $Na_v1.5$ improves predictivity of hERG data in respect of arrhythmia risk (33). Consequently, we performed additional experiments to test effects of CONA-437 on these two channels. CONA-437 at up to 30 μM did not produce any statistically significant effect on I_{Na} (11.9 μ3.8% change at 30 μM, n=4, *Fig. 8a*; P>0.05 against no change), or L-type Ca^{2+} channel activity (at 30 μM 103.5 ± 1.8% of control activity, n=4, *Fig. 8b*; P>0.05 against no change to control activity). By contrast, the positive control propafenone produced a concentration-dependent inhibition of $Na_v1.5$ current (IC_{50} of 1.3 μM and n_H of 0.9; *Fig. 8a*), and nifedipine demonstrated an inhibition of L-type Ca^{2+} channel activity in a concentration-dependent manner (with an IC_{50} of 8.7 nM and n_H of 1.1; *Fig. 8b*).

DISCUSSION

Serotonin can produce marked modulation of neuronal activity and neuronal targets for serotonin continue to be identified (34). In this study we have focused not on serotonin itself, but rather on a novel investigative SSRI, CONA-437, demonstrating and characterising the mechanism of acute block of hERG channels by this compound. We found that, under similar conditions, CONA-437 exhibits a similar potency against hERG to a previously reported SSRI, fluvoxamine (2.42 μM and 3.8 μM, respectively) (16), a potency which is broadly comparable to those

seen for other SSRIs - citalopram (14) and fluoxetine (15, 35), also studied in mammalian expression systems. Fluoxetine has also been reported to inhibit hERG channel trafficking (15, 35). Data for fluvoxamine on hERG trafficking are not available and the focus of the present study (on acute pharmacological actions on I_{hERG}) precluded the study of CONA-437 in this regard. It has been suggested that both experimental temperature and voltage-clamp waveform profile can influence the observed potency of I_{hERG} blockade (25, 27, 28). However, recording temperature did not significantly alter potency of CONA-437 (22°C: 0.99 μM; 35°C: 1.34 μM). Moreover, the use of different voltage protocols to elicit hERG currents did not have a statistically significant effect on potency (VAP 0.72 μM versus step-ramp 1.34 μM; VAP 0.72 μM versus step-step 2.42 μM): the observed shifts (~3-fold) were small in comparison to some agents previously studied (25, 27, 28). With tritiated tryptamine as serotonin transporter substrate, CONA-437 inhibits the human serotonin reuptake inhibitor expressed in HEK 293 cells with an IC_{50} of ~7 nM (Pfizer Inc, unpublished), which is markedly (~100-fold) less than the hERG IC_{50} with any protocol studied here; however, the compound's effects on other monoamine transporters occur at concentrations at which substantial hERG blockade would be anticipated (IC_{50} for human norepinephrine transporter of 6.5 μM and for human dopamine transporter of >40 μM; Pfizer Inc, unpublished). Structurally diverse compounds can have off-target effects that involve unexpected actions on Na^+ or Ca^{2+} channels (36, 37). For drugs that produce hERG/I_{Kr} K^+ channel inhibition, accompanying pharmacological effects on Na^+ or Ca^{2+} channels can, in principle, mitigate hERG/I_{Kr} blockade (33). However, our experiments showed that CONA-437 at up to 30 μM had no significant effect on $Na_v1.5$ current or L-type Ca^{2+} channel activity and thus the drug's effect on I_{Kr} is not likely to be balanced by concomitant actions on opposing inward currents (33).

Strong protocol-dependence of I_{hERG} blockade has been reported for drugs that exhibit marked use-dependent blocking kinetics (25, 29). For example, under similar conditions to the present study cisapride was found to exhibit IC_{50} values that varied ~10-fold between ventricular AP and step protocols (25). CONA-437 differs from cisapride in exhibiting much more rapidly developing blockade on membrane depolarisation and this characteristic of the drug's action is likely to minimise the influence on inhibitory potency of different voltage stimulus waveforms. The observation that CONA-437 produces significant I_{hERG} inhibition with very brief (30 ms) membrane depolarisation is comparable to prior data for fluvoxamine (16) and indicates considerably faster onset of action than reported for either citalopram or fluoxetine (13, 14). Collectively, our data provide evidence that, similar to fluvoxamine (16), CONA-437 is likely to exhibit a mixed state-dependence of channel block. I_{hERG} inhibition by CONA-437 was weakly voltage-dependent: a ~5 mV leftward shift in the activation curve was observed and there was a significant accentuation of the magnitude of inhibition at more depolarised potentials. These findings would suggest that channel opening influences CONA-437 binding. Although the lack of a significant shift in voltage-dependence of inactivation suggests that CONA-437 did not act to stabilise hERG channel inactivation, the onset of inactivation appeared to be significantly accelerated by CONA-437 (*Fig. 6*). This suggests either that the transition rate between the open and inactive states is accelerated upon binding of CONA-437 to the channel, or that the apparent acceleration of inactivation reflects rapid development of open channel block during depolarisation. Thus, our data on WT I_{hERG} recorded in standard ECS suggest that CONA-437 exhibits rapid open hERG channel block, although a component of closed channel block cannot be ruled out, since very rapidly developing open channel block and closed channel block cannot readily be distinguished from one another (16, 38). The attenuation of CONA-437 blocking potency of I_{hERG} high $[K^+]_e$ may, however, suggest a predominantly open channel blocking mechanism: it is both suggestive of drug binding in/close to the ion conduction pathway and is consistent with reduced ability of the drug to bind to open channels through electrostatic repulsion or 'knock off' of CONA-437 from its binding site, when the direction of K^+ flux is inward and enhanced through raised $[K^+]_e$.

A striking aspect of the data in the present study is that I_{hERG} blockade by CONA-437 was only modestly affected by mutation of the S6 residues Y652A and F656A. These residues in the S6 region of the channel constitute key components of the canonical drug binding site on the hERG channel as, for almost all hERG-blocking drugs tested to date, mutation of one or both of these residues has caused either a complete or a dramatic attenuation of blockade (8, 9). For example, the I_{hERG} blocking potency of the high affinity blocker MK-499 was decreased by 94- and 650-fold by Y652A and F656A respectively, with cisapride and terfenadine also reported to be highly sensitive (39). The potency of chloroquine was reduced approximately 500-fold by each mutation (40) and a number other drugs including (amongst others) fluoxetine (15), lidoflazine (21), clemastine (22), E-4031 and dofetilide (41), ibutilide and clofilium (42), are highly sensitive to mutation of one or both of these residues.

The SSRI fluvoxamine has been considered to be an exception amongst I_{hERG} blockers in that Y652A and F656A mutations only partially attenuate I_{hERG} carried by these mutant channels at drug concentrations that produce profound inhibition of WT I_{hERG} (16). In this study, we estimated the IC_{50} of CONA-437 for the block of Y652A and F656A channels to be raised ~3–4 fold compared to WT-hERG. This reduction in potency is rather modest compared to that occurring for the majority of hERG blockers studied previously, suggesting that - as for the structurally distinct SSRI fluvoxamine - neither Y652 nor F656 is an obligatory component of the drug binding site. Obligatory components of the drug binding site on the hERG channel for CONA-437 therefore remain to be elucidated. Interestingly, both fluvoxamine and a dronedarone (a benzofuran I_{hERG} blocker, the action of which is also relatively insensitive to mutation of Y652 and F656 (32)) share in common with CONA-437 the property of attenuated I_{hERG} block in high $[K^+]_e$ conditions. This may indicate that binding in/near the ion conduction pathway (most likely in the channel's inner cavity, rendered accessible on channel gating) can occur without a critical dependence on either Y652 or F656. A detailed understanding of the molecular determinants of I_{hERG} blockade is of prime importance if, in the future, hERG inhibition is to be avoided early during the drug design and development process (8). CONA-437 may therefore provide a useful pharmacological tool for future studies, in order better to understand how some agents can exert rapidly developing I_{hERG} inhibition by interacting with the channel without a critical dependence on the Y652 or F656 residues.

Acknowledgements: The authors would like to thank Lesley Arberry for excellent technical assistance.

Conflict of interests: This work was funded by Pfizer Global Research and Development.

REFERENCES

1. Shah RR. Drug-induced QT interval prolongation-regulatory guidance and perspectives on hERG channel studies. Novartis Found Symp 2005; 266: 251-280.
2. Yap YG, Camm AJ. Drug induced QT prolongation and torsades de pointes. *Heart* 2003; 89: 1363-1372.
3. Gintant GA. Preclinical Torsades-de-Pointes screens: advantages and limitations of surrogate and direct

approaches in evaluating proarrhythmic risk. *Pharmacol Ther* 2008; 119: 199-209.
4. Hancox JC, McPate MJ, El Harchi A, Zhang YH. The hERG potassium channel and hERG screening for drug-induced torsades de pointes. *Pharmacol Ther* 2008; 119: 118-132.
5. Friedrichs GS, Patmore L, Bass A. Non-clinical evaluation of ventricular repolarization (ICH S7B): results of an interim survey of international pharmaceutical companies. *J Pharmacol Toxicol Methods* 2005; 52: 6-11.
6. Sanguinetti MC, Jiang C, Curran ME, Keating MT. A mechanistic link between an inherited and an acquired cardiac arrhythmia: HERG encodes the I_{Kr} potassium channel. *Cell* 1995; 81: 299-307
7. Trudeau MC, Warmke JW, Ganetzky B, Robertson GA. HERG, an inward rectifier in the voltage-gated potassium channel family. *Science* 1995; 269: 92-95.
8. Sanguinetti MC, Mitcheson JS. Predicting drug-hERG channel interactions that cause acquired long QT syndrome. *Trends Pharmacol Sci* 2005; 26: 119-124.
9. Sanguinetti MC, Tristani-Firouzi M. hERG potassium channels and cardiac arrhythmia. *Nature* 2006; 440: 463-469.
10. Witchel HJ, Hancox JC, Nutt DJ. Psychotropic drugs, cardiac arrhythmia, and sudden death. *J Clin Psychopharmacol* 2003; 23: 58-77.
11. Pacher P, Kecskemeti V. Cardiovascular side effects of new antidepressants and antipsychotics: new drugs, old concerns? *Curr Pharm Des* 2004; 10: 2463-2475.
12. Sala M, Coppa F, Cappucciati C, *et al.* Antidepressants: their effects on cardiac channels, QT prolongation and Torsade de Pointes. *Curr Opin Investig Drugs* 2006; 7: 256-263.
13. Thomas D, Gut B, Wendt-Nordahl G, Kiehn J. The antidepressant drug fluoxetine is an inhibitor of human ether-a-go-go related gene (HERG) potassium channels. *J Pharm Exp Ther* 2002; 300: 534-548.
14. Witchel HJ, Pabbathi VK, Hofmann G, Paul AA, Hancox JC. Inhibitory actions of the selective serotonin re-uptake inhibitor citalopram on HERG and ventricular L-type calcium currents. *FEBS Lett* 2002; 512: 59-66.
15. Rajamani S, Eckhardt LL, Valdivia CR, *et al.* Drug-induced long QT syndrome: hERG K^+ channel block and disruption of protein trafficking by fluoxetine and norfluoxetine. *Br J Pharmacol* 2006; 149: 481-489.
16. Milnes JT, Crociani O, Arcangeli A, Hancox JC, Witchel HJ. Blockade of HERG potassium currents by fluvoxamine: incomplete attenuation by S6 mutations at F656 or Y652. *Br J Pharmacol* 2003; 139: 887-898.
17. Kiehn J, Lacerda AE, Wible B, Brown AM. Molecular physiology and pharmacology of HERG. Single channel currents and block by dofetilide. *Circulation* 1996; 94: 2572-2579.
18. Snyders DJ, Chaudhary A. High affinity open channel block by dofetilide of HERG expressed in a human cell line. *Mol Pharmacol* 1996; 49: 949-955.
19. Alexandrou AJ, Milnes JT, Leaney JL, *et al.* The impact of voltage-clamp protocol on the apparent potency of a rapidly acting human ether-a-go-go related gene (hERG) potassium channel blocker. *J Physiol* 2005; 567P: PC25.
20. Zhou Z, Gong Q, Ye B, *et al.* Properties of HERG channels stably expressed in HEK 293 cells studied at physiological temperature. *Biophys J* 1998; 74: 230-241.
21. Ridley JM, Dooley PC, Milnes JT, Witchel HJ, Hancox JC. Lidoflazine is a high affinity blocker of the HERG K^+ channel. *J Mol Cell Cardiol* 2004; 36: 701-705.
22. Ridley JM, Witchel HJ, Hancox JC. Witchel HJ. Clemastine, a conventional antihistamine, is a high potency inhibitor of the HERG K^+ channel. *J Mol Cell Cardiol* 2006; 40: 107-118.
23. Barry PH. JPCalc, a software package for calculating liquid junction potential corrections in patch-clamp, intracellular, epithelial and bilayer measurements and for correcting junction potential measurements. *J Neurosci Methods* 1994; 51: 107-116.
24. Alexandrou AJ, Duncan RS, Sullivan A, *et al.* Mechanism of hERG K^+ channel blockade by the fluoroquinolone antibiotic moxifloxacin. *Br J Pharmacol* 2006; 147: 905-916.
25. Milnes JT, Witchel HJ, Leaney JL, Leishman DJ, Hancox JC. Investigating dynamic protocol-dependence of hERG potassium channel inhibition at 37°C: cisapride versus dofetilide. *J Pharmacol Toxicol Methods* 2010; 61: 178-191.
26. Carmeliet E. Voltage- and time-dependent block of the delayed rectifier K^+ current in cardiac myocytes by dofetilide. *J Pharmacol Exp Ther* 1992; 262: 809-817.
27. Kirsch GE, Trepakova ES, Brimecombe JC, *et al.* Variability in the measurement of hERG potassium channel inhibition: effects of temperature and stimulus pattern. *J Pharmacol Toxicol Methods* 2004; 50: 93-101.
28. Yao JA, Du X, Lu D, Baker RL, Daharsh E, Atterson P. Estimation of potency of HERG channel blockers: impact of voltage protocol and temperature. *J Pharmacol Toxicol Methods* 2005; 52: 146-153.
29. Stork D, Timin EN, Berjukow S, *et al.* State dependent dissociation of HERG channel inhibitors. *Br J Pharmacol* 2007; 151: 1368-1376.
30. Ferreira S, Crumb WJ, Jr., Carlton CG, Clarkson CW. Effects of cocaine and its major metabolites on the HERG-encoded potassium channel. *J Pharmacol Exp Ther* 2001; 299: 220-226.
31. Wang S, Morales MJ, Liu S, Strauss HC, Rasmusson RL. Modulation of HERG affinity for E-4031 by $[K+]_o$ and C-type inactivation. *FEBS Lett* 1997; 417: 43-47.
32. Ridley JM, Milnes JT, Witchel HJ, Hancox JC. High affinity HERG K^+ channel blockade by the antiarrhythmic agent dronedarone: resistance to mutations of the S6 residues Y652 and F656. *Biochem Biophys Res Comm* 2004; 325: 883-891.
33. Kramer J, Obejero-Paz CA, Myatt G, *et al.* MICE models: superior to the HERG model in predicting Torsade de Pointes. *Sci Rep* 2013; 3: 2100. doi: 10.1038/srep02100.
34. Palus K, Chrobok L, Lewandowski MH. Depolarization of the intergeniculate neurons by serotonin - in vitro study. *J Physiol Pharmacol* 2013; 64: 773-778.
35. Wible BA, Hawryluk P, Ficker E, Kuryshev YA, Kirsch G, Brown AM. HERG-Lite: a novel comprehensive high-throughput screen for drug-induced hERG risk. *J Pharmacol Toxicol Methods* 2005; 52: 136-145.
36. Baylie RL, Cheng H, Langton PD, James AF. Inhibition of cardiac L-type calcium channel current by the TRPM8 agonist, (-)-menthol. *J Physiol Pharmacol* 2010; 61: 543-550.
37. Szentandrassy N, Papp F, Hegyi B, Bartok A, Krasznai Z, Nanasi PP. Tetrodotoxin blocks native cardiac L-type calcium channels but not Cav1.2 channels expressed in HEK cells. *J Physiol Pharmacol* 2013; 64: 807-810.
38. Mitcheson JS. Drug binding to HERG channels: evidence for a 'non-aromatic' binding site for fluvoxamine. *Br J Pharmacol* 2003; 139: 883-884.
39. Mitcheson JS, Chen J, Lin M, Culberson C, Sanguinetti MC. A structural basis for drug-induced long QT syndrome. *Proc Natl Acad Sci USA* 2000; 97: 12329-12333.
40. Sanchez-Chapula JA, Navarro-Polanco RA, Culberson C, Chen J, Sanguinetti MC. Molecular determinants of voltage-dependent human ether-a-go-go related gene (HERG) K^+ channel block. *J Biol Chem* 2002; 277: 23587-23595.
41. Kamiya K, Niwa R, Mitcheson JS, Sanguinetti MC. Molecular determinants of HERG channel block. *Mol Pharmacol* 2006; 69: 1709-1716.

42. Perry MD, deGroot MJ, Helliwell R, *et al.* Structural determinants of HERG channel block by clofilium and ibutilide. *Mol Pharmacol* 2004; 66: 240-249.

Received: September 17, 2011
Accepted: April 22, 2014

Author's address: Dr. Joanne Leaney, Discovery Park House, Ramsgate Road, Sandwich, Kent, Kent, CT13 9NJ, United Kingdom; E-mail: Joanne.Leaney@pfizer.com

and Prof. Jules Hancox, School of Physiology and Pharmacology, and Cardiovascular Research Laboratories, School of Medical Sciences, University Walk, Bristol, BS8 1TD, United Kingdom; E-mail: jules.hancox@bristol.ac.uk